JOURNAL OF SOLID STATE CHEMISTRY **123,** 14–20 (1996)
ARTICLE NO. 0146

Oxygen Vacancies in Pyrochlore Oxides: Powder Neutron Diffraction Study of $Pb_2Ir_2O_{6.5}$ and $Bi_2Ir_2O_{7-y}$

Brendan J. Kennedy

School of Chemistry, University of Sydney, Sydney NSW 2006, Australia

Received August 21, 1995; in revised form December 4, 1995; accepted December 7, 1995

The structure of the oxygen deficient pyrochlores $Bi_2Ir_2O_{7-y}$ and $Pb_2Ir_2O_{6.5}$ were refined by Rietveld analysis of time-of-flight neutron powder diffraction data. The diffraction data for $Pb_2Ir_2O_{6.5}$ have been used to refine the structure in the cubic space group $F\bar{4}3m$, $a = 10.26450(4)$ Å in which there is oxygen vacancy ordering and where each Pb atom is displaced 0.04 Å toward its associated vacancy. For $Bi_2Ir_2O_{7-y} = 0.2$ the structure was fitted within space group $Fd3m$, $a = 10.3256(1)$ Å, in which the oxygen vacancies are randomly distributed over the O′ sites. In both structures the Ir atoms are in a nearly regular octahedral coordination whereas the Bi and Pb cations have a distorted eightfold coordination, compressed scalehedron, geometry. XPS studies indicate there is appreciable surface enrichment of the *A* cation.

INTRODUCTION

Following on from early studies by Horowitz and co-workers (1–3) pyrochlore-type oxides of the type $A_2B_2O_{7-y}$ (A = Pb, Bi, B = Ru, Ir) are under active investigation in a number of laboratories for use as oxygen transfer catalysts for a variety of processes including O_2 reduction and evolution and for the oxidation of organic molecules (4–10). Recent results by Kannan *et al.* (4) and Goodenough and co-workers (5) demonstrate that the Ir pyrochlores are more stable oxygen reduction catalysts than the analogous Ru pyrochlores. This is some what surprising since the mechanism proposed by Goodenough *et al.* (5) for oxygen reduction involves only the A cations. It has been suggested that oxygen nonstoichiometry is critical in determining the activity and stability of these pyrochlore-type oxides, and a further difference between the two materials is possibly the extent and nature of the oxygen nonstoichiometry. The cubic pyrochlore structure is in space group $Fd3m$(No. 227) and has the larger A cation at 16*d* site (0.5, 0.5, 0.5), the smaller B cation at 16*c* (0,0,0), the O anion at 48*f* (x, 0.125, 0.125), and the O′ anion at 8*b* (0.375, 0.375, 0.375). For $Pb_2Ru_2O_{6.5}$ half the O′ sites are vacant, whereas there is some controversy about the precise oxygen stoichiometry in the analogous Ir pyrochlore. Stoichiometries of $Pb_2Ir_2O_{6.1}$–$Pb_2Ru_2O_{6.5}$ have been reported (11–14). The predisposition to oxygen nonstoichiometry in pyrochlores can be rationalized by considering the structure to exist as two interpenetrating B_2O_6 and A_2O' networks (15). The B cations are located at the center of corner-sharing oxygen octahedra. The A_2O' sublattice can be viewed as either as a network of corner-sharing A_4O' tetrahedra or as a system of $-A-O'-A-$ cuprite like chains. These two networks are only weakly interacting; neither the A or O′ ions are necessary to stabilize the basic pyrochlore structure.

Both $Pb_2Ir_2O_{6.5}$ and $Bi_2Ir_2O_{7-y}$ are good electrical conductors (10 to 1000 $\Omega\,cm^{-1}$) (13, 14, 16) as a consequence of the formation of an Ir–O conduction band. By comparison with results for the better studied ruthenium pyrochlores it is believed that the width and the splitting of the Ir–O states is dependent on the –Ir–O–Ir– overlap and on the A cation. Decreasing the Ir–O–Ir angle is expected to reduce the conductivity, although this appears to be moderated by the presence of vacancies in the A_2O' sublattice (17). For both Pb and Bi the empty *s* orbitals, which have about the same energy as *d* band, broaden the conduction band, thus enabling good electrical conductivity.

It has been shown that substitution of the A cation into the B sites in Pb and Bi pyrochlores can occur (2), and if this does happen then a reduction in conductivity should result since the A cations cannot provide electrons to the conduction band. Indeed it has been proposed by Goodenough and co-workers that substitution of Pb onto the B site in $Pb_2Ir_2O_{6.5}$ is commonplace (11). In principle powder neutron diffraction methods should be capable of determining if site substitution occurs.

As part of a detailed study of the structural and electrocatalytic properties of metal pyrochlores, it was decided to investigate the structure of $A_2Ir_2O_{7-y}$, A = Pb, Bi. The aim of the present work is threefold:

1. To obtain an accurate description of the structure of $A_2Ir_2O_{7-y}$, so to establish if oxygen vacancy ordering occurs and if there is any systematic variation in the Ir–O–Ir contacts.

0022-4596/96 $18.00

2. Identify any structural or electronic changes associated with exchanging Ir for Ru in pyrochlore oxides.

3. Use X-ray photoelectron spectroscopy to probe the electronic structures of the materials and to determine the surface properties of these.

EXPERIMENTAL

Polycrystalline samples of $A_2Ir_2O_{7-y}$ were prepared by the solid state reaction of stoichiometric amounts Bi_2O_3 or PbO and IrO_2 (Aldrich) at 600°C for 12 h, 800°C for 24 h, and 1050°C or 48 h with regrinding between successive firings. Only peaks due to the desired pyrochlore phase were observed in powder X-ray diffraction patterns recorded on a Siemens D-5000 diffractometer.

Time-of-flight (TOF) neutron powder diffraction data were collected on the POLARIS diffractometer at ISIS, Rutherford Appleton Laboratory. The sample (ca. 5 g) was contained in a vanadium can. Data collection required about 8 h. No precautions to avoid preferred orientation were taken. As a consequence of the high neutron absorption cross section of iridium the raw data were corrected for absorption. The TOF diffraction data from the back scattering bank of detectors (c bank) were analyzed by Rietveld profile analysis using the program GSAS (18). The TOF profile function used was a convolution of two back-to-back exponentials with a Gaussian. The Rietveld refinement was performed using all data points with *d* spacings between 0.325 and 3.2 Å (TOF 2–19.5 ms).

Atomic positions and anisotropic thermal parameters of the pyrochlore phase were refined simultaneously with the background and profile coefficients. The final *R* values were R_p 5.67, R_{wp} 5.56, and R_{exp} 3.44 and R_p 5.08, R_{wp} 5.40, and R_{exp} 2.33 for the Bi and Pb oxides, respectively. Coherent scattering lengths used were Pb 0.9401, Bi 0.8533, Ir 1.0600, and O 0.5805 fm.

X-ray photoelectron spectra were recorded on a Kratos XSAM 800 spectrometer using Mg$K\alpha$ radiation (1253.6 eV) at 15 kV, 12 mA with a constant pass energy of 20 eV. All binding energies are referenced to the C 1*s* signal at 284.6 eV. Spectra were analyzed using mixed Gaussian–Lorentzian (50:50) peak shapes and a linear background (19).

RESULTS AND DISCUSSION

The neutron diffraction refinement of the structure of $Bi_2Ir_2O_{7-y}$ in space group *Fd3m* proceeded without incident and confirms the material adopts a regular pyrochlore structure with $a = 10.3256(1)$ Å. The final positional thermal and occupancy parameters are given in Table 1. The agreement between the observed and calculated profiles is shown in Fig. 1. No 420 reflection was observed in the powder neutron or X-ray diffraction data, indicating that vacancy ordering on the O′ site has not ocurred (2). Refinement of occupancies of both the Bi and O′ sites indicated small deviations from the expected stoichiometry, the refined stoichiometry being $Bi_{1.9}Ir_2O_{6.8}$. This indicates that the small loss of Bi is compensated by the formation of vacancies at the O′ site and that there is no oxidation of Ir above the +4 oxidation state. Analytical electron microscopy studies revealed no unusal features or deviations from the expected stiochiometry. Attempts to place some Bi onto the Ir sites invariably lead to a worsening of the fit.

TABLE 1
Refined Structural and Thermal Parameters (10^{-2} Å^2) for $Bi_2Ir_2O_{7-y}$ at Room Temperature ($a = 10.3256(1)$ Å, Space Group *Fd3m*)

	Site	*x*	*y* = *z*	*N*	U_{11}	$U_{22} = U_{33}$	$U_{12} = U_{13}$	U_{23}
Bi	16*d*	0.5	0.5	0.956(5)	1.11(1)	$=U_{11}$	−0.27(1)	$=U_{12}$
Ir	16*c*	0	0	1	0.21(1)	$=U_{11}$	−0.01(1)	$=U_{12}$
O	48*f*	0.32985(4)	0.125	1	0.48(1)	0.50(1)	0	0.30(1)
O′	8*b*	0.375	0.375	0.815(11)	1.44(4)	$=U_{11}$	0	0

The cubic lattice parameter of $Bi_2Ir_2O_7$ 10.3256 Å is slightly larger than that found for the analogous bismuth ruthanate, $Bi_2Ru_2O_7$, $a = 10.2957$ Å (20) in accord with the slightly larger ionic radii of Ir^{4+} 0.68 Å compared to Ru^{4+} 0.62 Å. The Ir–O distance of 2.003(1) Å compares favorably with that found for other Ir(IV) oxides such as IrO_2, Ir–O_{av} 1.985 Å (21), and is slightly longer than the Ru–O distance of 1.974 Å found in $Bi_2Ru_2O_{6.9}$. Comparison with results recently obtained (22) for the series of stannate pyrochlores $Ln_2Sn_2O_7$ in which it was found that the unique oxygen positional parameter, *x*, systematically decreases as the cubic lattice parameter increases suggests that the positional parameter in $Bi_2Ir_2O_7$ should be smaller than that observed for $Bi_2Ru_2O_7$. In fact the opposite is observed; the refined positional parameter for the O atoms are 0.32985(4) and 0.3266(1) for the Ir and Ru compounds, respectively. The altered value of the oxygen positional parameter presumably arises from the strong *M*–*M* interactions in these metallic oxides. The higher value of *x* found for $Bi_2Ir_2O_{7-y}$ results in a decrease in the *B*–O–*B* angle to 131.38(2)° from 133.14° in $Bi_2Ru_2O_{7-y}$. To a first approximation this may be taken as evidence of weaker *B*–O–*B* interactions in $Bi_2Ir_2O_7$ (23), however this neglects the fact the Ir 5*d* orbitals are more diffuse so that strong overlap of the Ir–O orbitals is still possible. Indeed, $Bi_2Ir_2O_7$ is reported (16) to have a negative temperature resistivity coefficient (TRC) indicative of a metallic oxide, whereas $Bi_2Ru_2O_7$ has a very slightly positive TRC (2).

The BiO_8 scalenohedron is axially compressed in both the Ru and Ir pyrochlores; in the Ir compound there are six oxygen atoms at Bi–O 2.5335(2) and two at 2.2356(3)

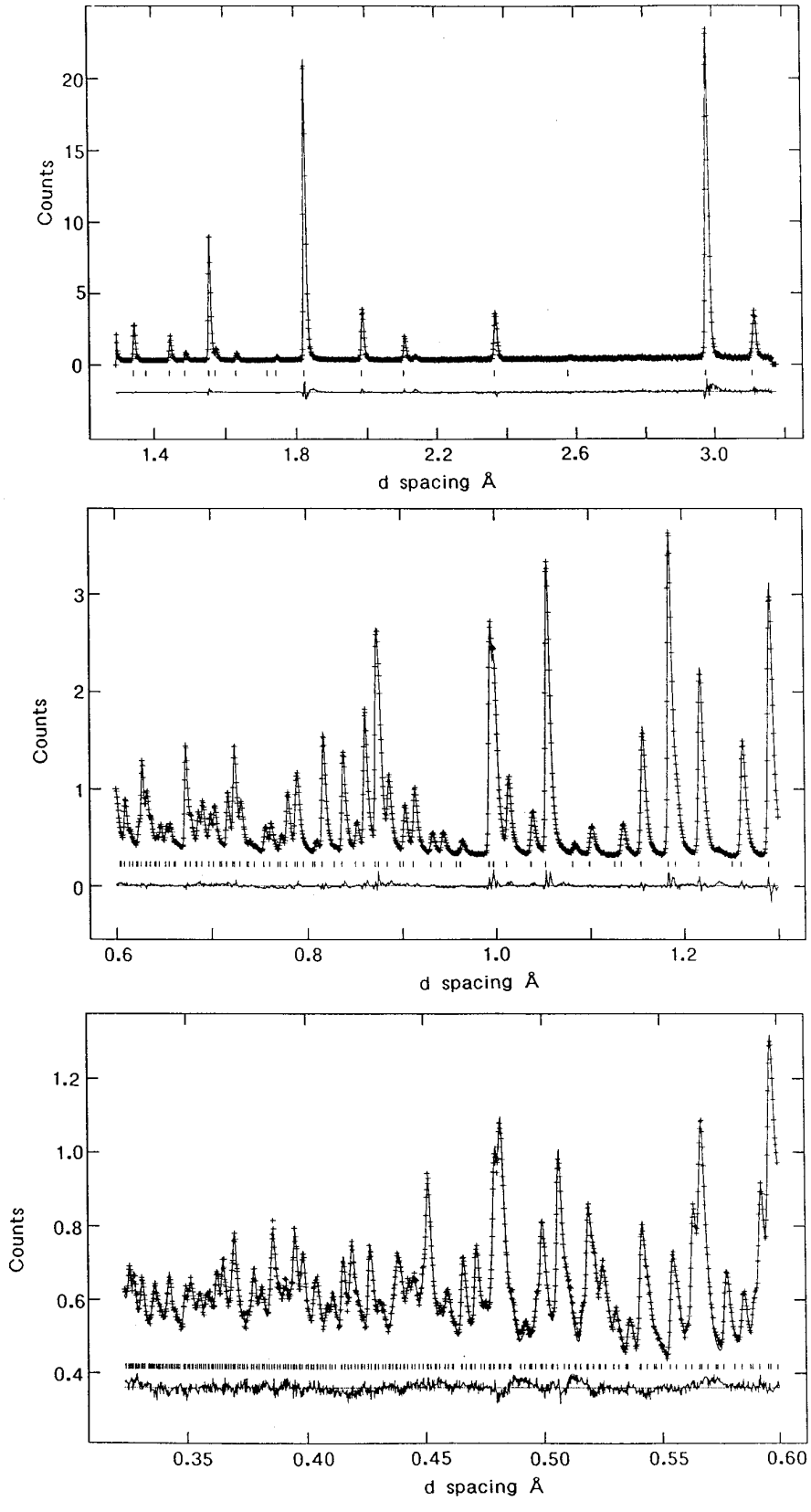

FIG. 1. Observed, calculated, and difference neutron powder diffraction profiles for $Bi_2Ir_2O_{7-y}$. The short vertical lines below the profiles mark the position of all possible Bragg reflections.

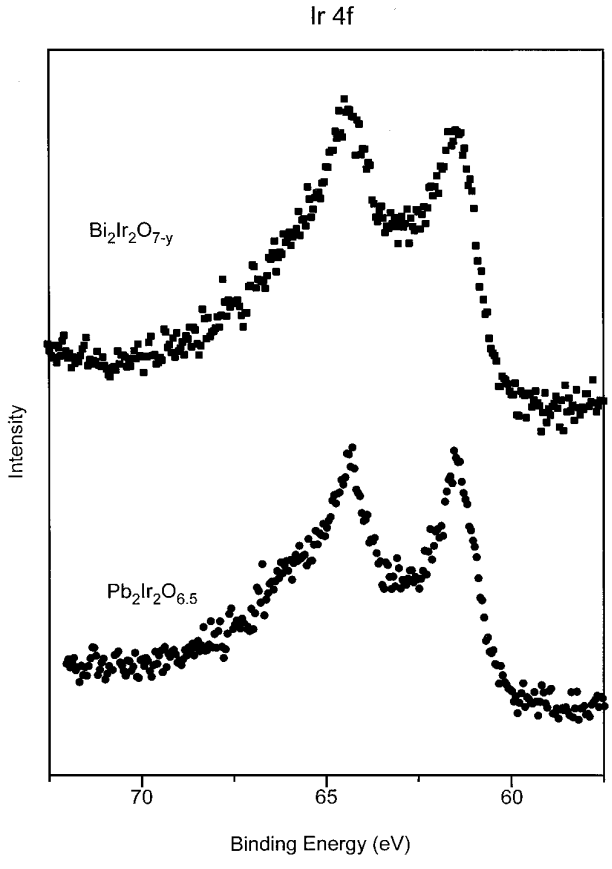

FIG. 2. Ir 4*f* photoelectron spectra of $Bi_2Ir_2O_{y-y}$ and $Pb_2Ir_2O_{6.5}$.

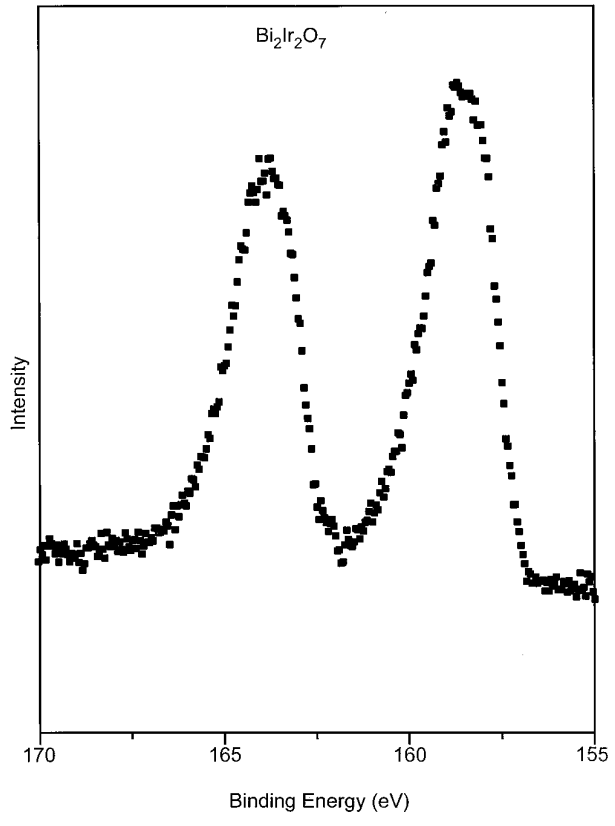

FIG. 3. Bi 4*f* photoelectron spectra of $Bi_2Ir_2O_{y-y}$ showing the broadening to higher binding energies as a consequence of electron screening and surface oxidation.

Å. These Bi–O bond lengths are similar to those found in $Bi_2Ru_2O_7$. The thermal parameters for both the Bi and O(1) atoms are large and highly anisotropic. For the Bi atom movement along the threefold axis, that is toward the two closest O atoms, is inhibited; the principal vibration is parallel to the [111] direction, is given by $U_{11} + 2U_{12} = 5.7 \times 10^{3-}$ Å^2, and is noticeably smaller than movements perpendicular to this direction, $U_{11} - U_{12} = 13.8 \times 10^{\times 3}$ Å^2. For the O(1) atom displacement in the (011) plane, $U_{22} - U_{23} = 2.0 \times 10^{-3}$ Å^2 is much smaller than that in the [100] $U_{11} = 4.8 \times 10^{-3}$ Å^2 or [011] $U_{22} + U_{23} = 8.0 \times 10^{-3}$ Å^2 directions.

A wide range survey X-ray photoelectron spectra of $Bi_2Ir_2O_{7-y}$ revealed no surface impurities. At higher resolution both the Bi 4*f* and Ir 4*f* XP spectral manifolds appear as asymmetric doublets, Figs. 2 and 3, which are best described by at least two doublets, albeit of dramatically different half widths (Table 2). Considering the Ir 4*f* spectra, the line near 63.9 eV is of greater intensity than that near 60.9 eV. While some small deviation in relative intensities from that predicted from simple multiplet theory is not unexpected, the spectra apparently consist of at least two Ir 4*f* doublets, the BE of the lower energy Ir $4f_{7/2}$ line at 60.9 eV being typical of an Ir(IV) oxide such as IrO_2. The higher BE line $4f_{7/2}$ line at 62.5 eV can then be ascribed to a higher oxidation state, the large half width suggesting that more than one such species is involved. Such a result is in contrast to the diffraction results which suggest that bulk formation of Ir(V) is not possible in the pyrochlores; although obviously this does not preclude formation of such surface species. The asymmetry of the Bi 4*f* manifold is noticeably less than that observed for the Ir 4*f* signal, however it was not possible to satisfactorily reproduce the

TABLE 2
XPS Data for the Iridium Pyrochlore Oxides

	A $4f_{7/2}$ (eV)	Δ^a	Γ^b	Ir $4f_{7/2}$ (eV)	Δ	Γ	*A* : Ir
$Bi_2Ir_2O_7$	157.61	5.31	1.3	60.86	3.03	1.1	65 : 35
	158.58	5.25	2.0				
$Pb_2Ir_2O_{6.5}$	136.37	4.85	1.1	60.84	2.96	1.1	62 : 38
	137.51	4.91	2.3				

[a] Separation between the Ir $4f_{7/2}$ and Ir $4f_{5/2}$ spin orbit doublets.
[b] Full width at high height for the peaks.

TABLE 3
Refined Structural and Thermal Parameters (10^{-3} Å^2) for $Pb_2Ir_2O_{6.5}$ at Room Temperature (a = 10.26450(4) Å, Space Group $F43m$)

	Site	x	$y = z$	N	U_{11}	$U_{22} = U_{33}$	$U_{12} = U_{13}$	U_{23}
Pb	16*e*	0.8775(1)	x	1	5.7(1)	$=U_{11}$	−0.1(1)	$=U_{12}$
Ir	16*e*	0.355(1)	x	1	2.3(1)	$=U_{11}$	−0.2(1)	$=U_{12}$
O	24*f*	0.2997(2)	0	1	5.7(1)	3.2(1)	0	−0.4(1)
O	24*g*	0.4522(2)	0.25	1	4.4(5)	5.9(4)	0	−4.9(4)
O′	4*a*	0.75	0.75	0.936(16)	3.6(4)	$=U_{11}$	0	0

spectra with a single doublet, the measure of fit being an unacceptably high 7.0%. Considering the spectra to consist of two doublets led to a reduction in R to 2.2%. In this case the lowest energy Bi $4f_{7/2}$ line at 157.6 eV is typical of a Bi(III) oxide and is comparable to the value found in $Bi_2Ru_2O_7$.

Quantification of the Bi : Ir surface composition demonstrates that the surface region is Bi rich, the ratio being 65 : 35 Bi : Ir. In part the asymmetry of the Bi 4*f* signal is thought to result from segregation of a Bi(III) oxide at the surface of the material (10). Unfortunately the materials are easily reduced precluding meaningful depth analysis by Ar^+ ion etching. Thus while it is possible that the higher BE components result from surface oxidation it is more likely that both the Bi and Ir 4*f* spectra are in fact asymmetrical as a consequence of screening of the core hole by the conduction electrons (24); in the case of Bi this is coupled with surface segregation. Presumably, since Bi_2O_3 is relatively nonvolatile, especially with respect to Ir oxides, the Bi resulting from the Bi deficiency exists as an amorphous surface oxide. There was no evidence to suggest that any surface rearrangement occurred during the measurements, nor was there any evidence of unusal features in a high resolution electron microscopy study of the sample.

Both the powder neutron and X-ray diffraction patterns of $Pb_2Ir_2O_{6.5}$ are typical of a cubic pyrochlore-type material, although on close examination a number of extra very weak lines were observed. The appearance of weak $hk0$ lines with $h + k \neq 4n$ (420,860) and $h00$ lines, with $h \neq$ (200), which are forbidden in space group $Fd3m$, is consistent with the loss of inversion symmetry at the cation sites, as occurs when the oxygen vacancies are ordered. Accordingly the profile refinement was performed in space group $F43m$ (No. 216) in which the cations can be displaced along [111]. Refined values for the positional, thermal, and occupational parameters are given in Table 3 and the best fit profile is shown in Fig. 4. Attempts to refine a model where Pb substitution onto the B cation site did not improve the fit, although in this case the relatively small difference between the scattering lengths of Ir and Pb indicates that it may be possible for a small amount of substitution to have occurred. The refined lattice parameter, 10.26450(4) Å, is in good agreement with previously reported values (11–14), although it is noticeably smaller than that found for $Bi_2Ir_2O_{7-y}$ despite the fact that the ionic radii of Pb^{2+}, at least for an octahedral geometry, is appreciably larger than that of Bi^{2+}, 1.19 vs 1.03 Å. Thus it appears that the lattice parameter is unexpectedly small effectively limiting the substitution of Pb^{4+} onto the Ir sites. Even small amounts of substitution of Pb^{4+} onto the Ir^{4+} sites is expected to increase the cubic lattice parameter.

The refined values for the Pb and Ir atom positions at 16*e* (x, x, x) $x_{Pb} = 0.8775(1)$ and $x_{Ir} = 0.3755(1)$ show that the Pb has been displaced significantly from the $Fd3m$ inversion symmetry position $x_{Pb} = 0.875$, moving 0.044(1) Å toward its assocaited vacancy so that along the [111] direction the Pb–vacancy distance is 2.178 Å while the Pb–O distance is 2.267 Å. The longer Pb–O distances are 2.546 Å. The Ir atom has not been significantly shifted from the position found in the $Fd3m$ model moving only 0.009(2) Å. The two Ir–O bond distances are obviously smaller than those found for $Bi_2Ir_2O_{7-y}$, 1.968 and 1.985 Å, and appear typical of an Ir(IV) oxide, although it appears that the average Ir(V)–O bond distance is only slightly lower than that found for Ir(IV)–O bonds.

As found for the Bi iridate, the cubic lattice parameter of $Pb_2Ir_2O_{6.5}$ is slightly larger than that found (3) for $Pb_2Ru_2O_{6.5}$. Both the PB–vacancy and the Pb–O distances in the two oxygen deficient pyrochlores are essentially same. The Ir–O–Ir angle in $Pb_2Ir_2O_{6.5}$ is 133.26° which suggests the conductivity should be greater than that found in $Bi_2Ir_2O_{7-y}$ where it is 131.38° although it is still smaller than the 134.81 found for the analogous Ru–O–Ru contact in $Pb_2Ru_2O_{6.5}$. In fact, both $Bi_2Ir_2O_7$ and $Pb_2Ru_2O_{6.5}$ are metallic oxides with negative TPC whereas $Pb_2Ir_2O_{6.5}$ has a positive TCR albeit with a very low activation energy (2, 16). It is clear that while the B–O–B angles tend to be smaller in the Ir compounds relative to the Ru pyrochlores, the Ir oxides are good electrical conductors. A more systematic study of the influence of the B–O–B angles on conductivity in the iridate pyrochlores is required.

The Pb 4*f* and Ir 4*f* spectral manifolds in $Pb_2Ir_2O_{6.5}$ are reasonably similar to that seen for $Bi_2Ir_2O_7$; in this case the asymmetry of the Pb 4*f* doublet to higher BE is much more evident although the area of this second doublet is somewhat less (Fig. 5). The BE of the main Ir 4*f* doublet, Ir $4f_{7/2}$ = 60.8 eV, is indicative of an Ir(IV) oxide, while the shoulder to higher BE is indicative of a higher OS and/or screening. The Pb 4*f* spectra is insensitive to oxidation state changes; the Pb $4f_{7/2}$ line is at 138.4 eV in PbO_2 and 138.1 eV in PbO, although studies of electrochemically xoidized $Pb_2Ru_2O_{6.5}$ surfaces show that the BE of the bulk material is significantly lower than this and is readily distinguished from nonpyrochlore surface oxides. Again, while there is considerable surface depletion of Ir, the surface Pb : Ir ratio being 62 : 38, it is believed that the asymmetry

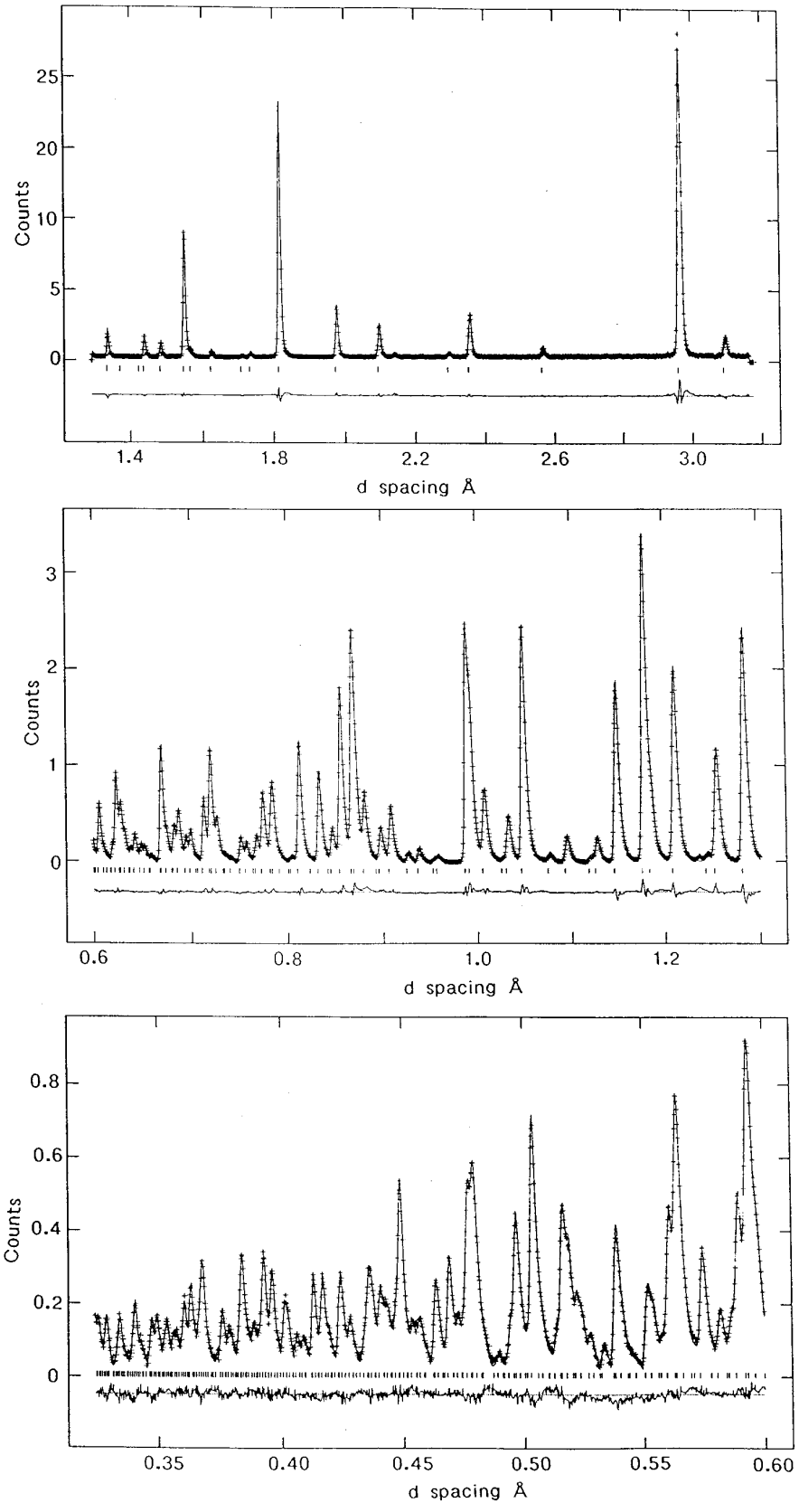

FIG. 4. Observed, calculated, and difference neutron powder diffraction profiles for $Pb_2Ir_2O_{6.5}$. The short vertical lines below the profiles mark the position of all possible Bragg reflections.

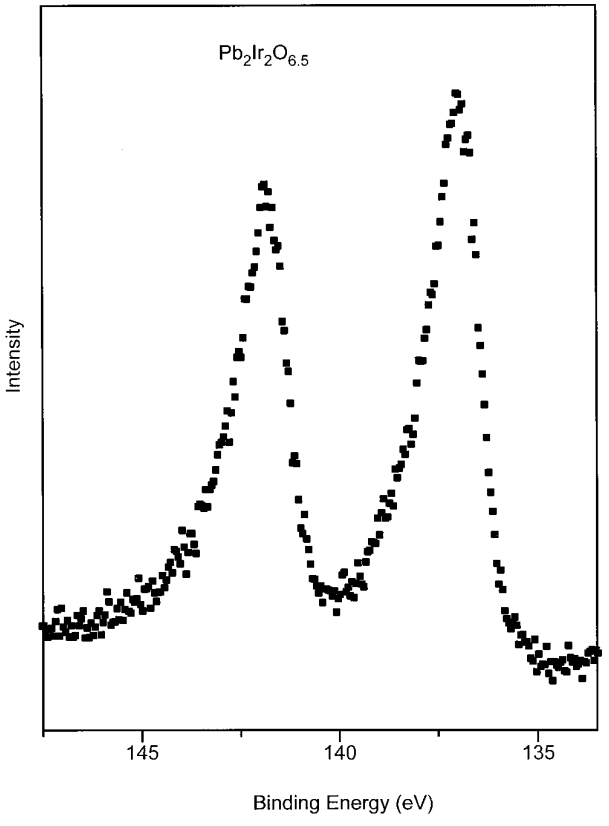

FIG. 5. Pb 4*f* photoelectron spectra of $Pb_2Ir_2O_{6.5}$ showing the broadening to higher binding energies as a consequence of electron screening and surface oxidation.

arises from a combination of screening effects and the formation of a surface Pb oxide.

To balance the valency in this material it is necessary that either 25% of the Pb on the *A* site is oxidized to Pb^{4+} or 50% of the Ir on the *B* site is present as Ir^{V}. Unfortunately, as a consequence of screening effects it is not possible to unequivocally identify all the OS present, however the weight of evidence from the structural analysis favors the latter model; i.e., the compound is a mixed valent ($Ir^{IV/V}$) compound.

The observation of surface enrichment by the *A* cation in both $Pb_2Ir_2O_{6.5}$ and $Bi_2Ir_2O_{7-y}$ coupled with the apparent formation of a second surface oxide in $A_2Ir_2O_{6-y}$ is in accord with Goodenough's model (5) for oxygen reduction on pyrochlore surfaces, where the initial step involves the displacement of OH ions at surface oxygen sites in the A_2O' sublattice. The oxygen of the Ir_2O_6 framework does not participate in this reaction, although it is central to the oxygen evolution process. Further studies of the changes in the surface chemistry of these and other Ir oxides are in progress and will be reported.

ACKNOWLEDGMENTS

The support of the Australian Research Council and the assistance of Drs. S. Hull and R. Smith at ISIS is gratefully acknowledged.

REFERENCES

1. H. S. Horowitz, J. M. Longo, and H. H. Horowitz, *J. Electrochem. Soc.* **130,** 1851 (1983).
2. R. A. Beyerlein, H. S. Horoqitz, and J. M. Longo, *J. Solid State Chem.* **72,** 2 (1988).
3. R. A. Beyerlein, H. S. Horowitz, J. M. Longo, M. E. Leonowicz, J. D. Jorgensen, and F. J. Rotella, *J. Solid State Chem.* **51,** 253 (1984).
4. A. M. Kannan, A. K. Shukla, and S. Sathyanarayana, *J. Electroanal. Chem.* **281,** 339 (1990).
5. J. B. Goodenough, R. Manoharan, and M. Paranthaman, *J. Am. Chem. Soc.* **112,** 2076 (1990).
6. L. Swette, N. Kackley, and S. A. McGatty, *J. Power Sources* **36,** 323 (1991).
7. R. G. Egdell, J. B. Goodenough, A. Hamnett, and C. C. Naish, *J. Chem. Soc., Faraday Trans I* **79,** 893 (1983).
8. T. R. Felthouse, P. B. Fraundorf, R. M. Friedman, and C. L. Schosser, *J. Catal.* **127,** 421 (1991).
9. G. Gokagac and B. J. Kennedy, *J. Electroanal. Chem.* **353,** 71 (1993).
10. G. Gokagac and B. J. Kennedy, *J. Electroanal. Chem.* **368,** 235 (1994).
11. J. M. Longo, P. M. Raccah, and J. B. Goodenough, *Mater. Res. Bull.* **4,** 191 (1969).
12. A. W. Sleight, *Mater. Res. Bull.* **6,** 775 (1971).
13. R. J. Bouchard and J. L. Gillson, *Mater. Res. Bull.* **6,** 669 (1971).
14. V. B. Lazarev and I. S. Sharplygin, *Russ. J. Inorg Chem.* **23,** 291 (1978).
15. M. A. Subramanian, G. Aravamudan, and G. V. Subba Rao, *Prog. Solid State Chem.* **15,** 55 (1983).
16. J. F. Vente, Ph. D. Thesis, The University of Leiden, 1994.
17. B. J. Kennedy, *J. Solid State Chem.* **119,** 254 (1995).
18. A. C. Larson and R. B. Von Dreele, "LANSCE General Structural Analysis System (MA-H805)." Los Alamos National Laboratory, Los Alamos, NM 87545, 1991.
19. Vision reference Manual, Kratos, UK.
20. G. R. Facer, M. M. Elcombe, and B. J. Kennedy, *Aust. J. Chem.* **46,** 1897 (1993).
21. A. A. Bolzan, C. Fong, B. J. Kennedy, and C. J. Howard, *Acta Crystallogr. B*, accepted (1996).
22. B. J. Kennedy, unpublished observations.
23. R. Kanno, Y. Takeda, T. Yamamoto, Y. Kawamoto, and O. Yamamoto, *J. Solid State Chem.* **102,** 106 (1993).
24. P. A. Cox, "Transition Metal Oxides" (OUP) 1992.